Parity violation in neutron resonances of palladium

D. A. Smith,[1,*] J. D. Bowman,[1] B. E. Crawford,[2,†] C. A. Grossmann,[3,‡] T. Haseyama,[4,§] A. Masaike,[4,‖] Y. Matsuda,[4,¶] G. E. Mitchell,[3] S. I. Penttila,[1] N. R. Roberson,[2] S. J. Seestrom,[1] E. I. Sharapov,[5] S. L. Stephenson,[3,†] and V. W. Yuan[1]

[1]*Los Alamos National Laboratory, Los Alamos, New Mexico 87545*

[2]*Duke University, Durham, North Carolina 27708*

and Triangle Universities Nuclear Laboratory, Durham, North Carolina 27708-0308

[3]*North Carolina State University, Raleigh, North Carolina 27695-8202*

and Triangle Universities Nuclear Laboratory, Durham, North Carolina 27708-0308

[4]*Physics Department, Kyoto University, Kyoto 606-01, Japan*

[5]*Joint Institute for Nuclear Research, 141980 Dubna, Russia*

(Received 3 November 2001; published 4 March 2002)

Parity violation in *p*-wave neutron resonances of the palladium isotopes 104, 105, 106, and 108 has been measured by transmission of a longitudinally polarized neutron beam through a natural palladium target. The measurements were performed at the pulsed spallation neutron source of Los Alamos Neutron Science Center. The rms weak interaction matrix elements and the corresponding spreading widths were determined for ^{104}Pd, ^{105}Pd, and ^{106}Pd.

DOI: 10.1103/PhysRevC.65.035503 PACS number(s): 24.80.+y, 11.30.Er, 25.40.Ny, 27.60.+j

I. INTRODUCTION

The earlier experimental approach to the study of parity nonconservation (PNC) in light nuclei involved the measurement of a parity violating observable (often a forbidden γ-ray transition), and the calculation of the strength of the parity violating transition between two states whose wave functions are calculated with the nuclear shell model. Unfortunately the results are very sensitive to the details of the wave functions. This approach is summarized in the classic review by Adelberger and Haxton [1]. The discovery of very large parity violation for neutron resonances in La, Sn, and Br by the Dubna group [2] and the subsequent time reversal invariance and parity at low energies (TRIPLE) measurements [3] in heavy nuclei led to a new, statistical approach to the study of parity violation in heavy nuclei. The symmetry-breaking matrix elements in compound nuclei are assumed to be random variables. The goal of the PNC experiments is to determine the root-mean-square symmetry-breaking matrix element. This weak matrix element is obtained from a set of longitudinal asymmetries measured for a number of resonances per nuclide. The key point is that the value of the rms matrix element can be obtained without detailed information about the wave functions. For a *p*-wave resonance at energy E, the longitudinal asymmetry p is defined by

$$\sigma^{\pm}(E)=\sigma_{\mathrm{p}}(E)(1\pm p), \tag{1}$$

where $\sigma^{\pm}(E)$ is the neutron cross section for the $+$ and $-$ neutron helicity states, and $\sigma_{\mathrm{p}}(E)$ is the *p*-wave resonance cross section for unpolarized neutrons.

The pulsed spallation neutron source at the Los Alamos Neutron Science Center (LANSCE) was very well suited for these experiments. Results from the initial TRIPLE measurements are discussed in reviews by Bowman *et al.* [3] and Frankle *et al.* [4]. A general theoretical review of the enhancement of parity and time-invariance violating effects in compound nuclei is given by Flambaum and Gribakin [5]. Following the preliminary measurements, the TRIPLE collaboration improved the experimental apparatus and developed an improved data analysis method. The early measurements were repeated, and many additional targets were investigated. A brief review with emphasis on the generic aspects of the parity violation enhancement is given by Mitchell, Bowman, and Weidenmüller [6]. A recent, comprehensive review is given by Mitchell *et al.* [7]

The parity violation measurements are practical only near a maximum of the *p*-wave neutron strength function. The TRIPLE measurements on ^{232}Th [8] and ^{238}U [9] are near the maximum of the $4p$ neutron strength function. To consider the possible mass dependence of the effective nucleon-nucleus weak interaction, we performed measurements in the $A=110$ mass region, where the $3p$ neutron strength function maximum is located. We have published results for several nuclei in this mass region: ^{93}Nb [10], ^{103}Rh [11], ^{107,109}Ag [12], ^{113}Cd [13], ^{115}In [14], ^{117}Sn [15], ^{121,123}Sb and ^{127}I [16], and ^{133}Cs [17]. Except for ^{93}Nb, parity violation effects were observed for all of the odd mass targets that we studied near the $3p$ neutron strength function maximum. The analysis of the parity violation data becomes much more complicated for targets with nonzero spin. Spectroscopic information (including spins) for the *s*- and *p*-wave resonances is very important. In the absence of this spectroscopic information, averages over the unknown parameters can be performed, but this averaging often leads to a large uncertainty in the value for the rms PNC matrix element.

*Present address: Stanford Linear Accelerator Center, Stanford, CA 94309.

†Present address: Gettysburg College, Gettysburg, PA 17325.

‡Present address: Avant! Corporation, Durham, NC 27703.

§Present address: Institute for Chemical Research, Kyoto University, Kyoto, 611-0011, Japan.

‖Present address: Fukui University of Technology, 3-6-1 Gakuen, Fukui-shi, 910-8505, Japan.

¶Present address: Institute of Physical and Chemical Research (RIKEN), Saitama, 351-0198, Japan.

Here we report on our PNC study on the palladium isotopes. Palladium has one odd mass isotope and several even isotopes. The odd isotope ^{105}Pd has a high level density as compared with the even isotopes. A large number of new resonances were observed in the transmission experiment with a natural target, but their assignment to a specific isotope required additional measurements. These measurements were performed with isotopically enriched targets and a γ-ray detector array [18]. In addition, many resonances that were not observed in the natural target due to overlapping resonances were clearly observed with the isotopically enriched targets. These spectroscopic results are described in a recent paper by Smith *et al.* [19]. Earlier PNC measurements on enriched ^{106}Pd and ^{108}Pd using the γ-ray detector array were reported by Crawford *et al.* [20]. In this paper we combine these earlier results with the results from the present transmission PNC measurement and the extensive spectroscopic measurements.

In Sec. II the experimental methods for the parity violation measurements are described. The experimental results are presented in Sec. III, while the analysis to obtain the longitudinal asymmetries is discussed in Sec. IV. The extraction of the PNC matrix elements and the weak spreading widths is described in Sec. IV and the results for the palladium isotopes are given in Sec. V. The final section presents a brief summary and conclusions.

II. EXPERIMENTAL METHOD

Measurement of the PNC asymmetries was performed at the Manuel Lujan Jr. Neutron Scattering Center. The pulsed spallation neutron source is described by Lisowski *et al.* [21]. The initial experimental system to measure PNC effects at LANSCE was developed by the TRIPLE Collaboration [22]. The flux monitor [23], the polarizer [24], the spin flipper [25], and the neutron detector [26] are described in separate papers. The polarized epithermal neutron beam line for the present PNC experiments is described in Ref. [12]. The measurements were performed on flight path 2, which views a gadolinium-poisoned water moderator and has a cadmium/boron liner to reduce the number of low-energy neutrons in the tail of the neutron pulse. The neutrons are then collimated to a 10-cm diameter beam inside a 5-m thick biological shield. A ^{3}He/^{4}He ion chamber system [23] is used as a flux monitor. The neutron flux is measured for each neutron burst. These flux measurements are used to normalize the detector rates. The neutrons then pass through a polarized-proton spin filter [24]. Due to the difference in the singlet and triplet n-p cross sections, neutrons with one of the two helicity states are preferentially scattered out of the beam. The longitudinally polarized neutron beam has a polarization of $f_n \simeq 70\%$. The neutron spin was reversed (every 10 s) by a spin reversal device consisting of a system of magnetic fields [25]. Approximately every two days the overall neutron spin direction was changed by reversing the polarization direction of the proton spin filter.

PNC effects in palladium were measured by transmitting the neutron beam through a sample located at the downstream part of the spin flipper. The cylindrical sample of natural palladium had an areal density of 5.40×10^{23} atoms/cm^2. The measurements were performed both at room temperature and at 77 K. The ^{10}B-loaded liquid scintillation detector [26] was 56.7 m from the neutron source. This detector has an efficiency of 95%, 85%, and 71% at neutron energies of 10 eV, 100 eV, and 1000 eV, respectively. The neutron mean capture time in the detector is 416 ± 5 ns.

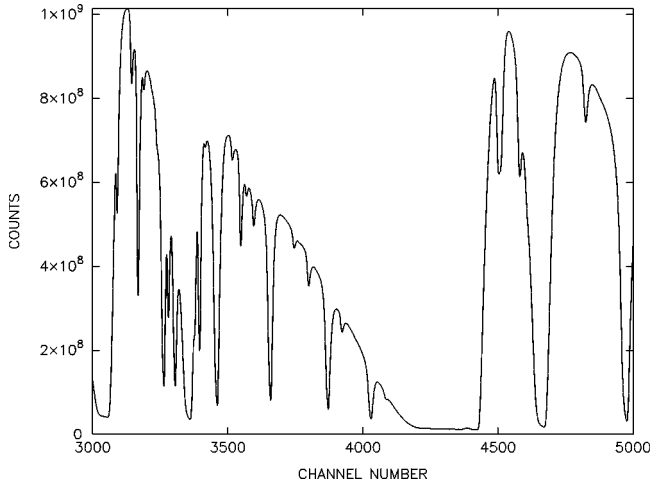

FIG. 1. The experimental neutron time-of-flight transmission spectrum for natural palladium for the energy region 60 eV to 160 eV.

The data acquisition process is initiated with each proton burst. After the detector signals are linearly summed and filtered, an analog to digital converter (ADC) transient recorder digitally samples the summed detector signal 8192 times in intervals determined by the filtering time. These 8192 words are added to a summation memory for 200 beam bursts before being stored. This process is repeated 160 times. This data set is treated as a unit for data analysis and corresponds to about a 30-minute ''run.'' For palladium 259 runs with a channel width of 100 ns were used in the final analysis.

III. EXPERIMENTAL DATA

The natural palladium time-of-flight (TOF) spectrum in the energy region approximately 60–160 eV is shown in Fig. 1. Many new resonances were observed in the transmission spectrum of the natural target and the assignment of these new resonances to a particular palladium isotope was a challenge. The stable isotopes of palladium are ^{102}Pd (1.02%), ^{104}Pd (11.14%), ^{105}Pd (22.33%), ^{106}Pd (27.33%), ^{108}Pd (26.46%), and ^{110}Pd (11.72%). Isotopic identification was achieved by a combination of measurements on isotopically enriched targets using the γ-ray detector. The details of this procedure and the final spectroscopic results are given by Smith *et al.* [19]. Resonance parameters were determined by analysis of the data summed over both helicity states. Background and dead time corrections were applied as described by Crawford *et al.* [9]. The shape analysis was performed with the code FITXS [27], which was written to analyze the TOF spectra measured by the TRIPLE collaboration. The

TABLE I. Resonance parameters and PNC asymmetries p for ^{104}Pd. The parameter A_J has dimensions eV^{-1}.

E (eV)	l	J	$g\Gamma_n$ (meV)	A_J	p (%)	$\lvert p\rvert/\Delta p$
109.7[a]	1		0.062 ± 0.006	1.7	0.08 ± 0.10	0.8
156.7[a]	1		0.024 ± 0.002			
182.4	0	0.5	297 ± 4			
266.6[a]	1		1.07 ± 0.10	0.45	-0.12 ± 0.03	4.0
294.5[a]	1		1.30 ± 0.13	0.33	0.01 ± 0.18	0.06
347.3[a]	0	0.5	15.7 ± 1.5			
522.0[a]	1		4.3 ± 0.4			
524.4[a]	1		2.0 ± 0.2			
607.5[a]	1		4.5 ± 0.5			
638.7[a]	1		7.8 ± 0.8			
678.9[a]	1		2.4 ± 0.3			
738.2[a]	1		2.7 ± 0.3			
769.2[a]	1		0.21 ± 0.02			
888.1[a]	1		7.2 ± 0.7			
935.0[a]	1		13.0 ± 1.2			
944.5[a]	0	0.5	700 ± 65			
994.9[a]	0	0.5	35.0 ± 3.2			
1178[a]	1		0.8 ± 0.3			

[a]New resonances.

multilevel, multichannel formalism of Reich and Moore [28] was used for the neutron cross sections, which were convoluted with the TOF resolution function developed by Crawford *et al.* [9]. The final fitting function is

$$\mathcal{F}_t(t)=\left\{B_t(t)\otimes\left[\frac{\alpha}{E^{0.96}}e^{-n\sigma_D(t)}\right]\right\}+\sum_{i=0}^{3}\frac{a_i}{t^i}, \qquad (2)$$

where σ_D(t) is the Doppler-broadened total cross section, $B_t(t)$ is the instrumental response function (which includes line broadening due to the initial width of the pulsed beam, neutron moderation, finite TOF channel width, and mean time for neutron capture in the detector), $\alpha/E^{0.96}$ is the energy-dependent neutron flux, and the second term represents a polynomial fit to the background. (The symbol $\otimes$ indicates a convolution.) The fitting procedure is described at length by Crawford *et al.* [9]. The neutron resonance energies, $g\Gamma_n$ widths, and radiative widths are obtained from this analysis. Resonance parameters for ^{104,105,106,108}Pd are listed in Tables I–IV.

After determining the resonance parameters, the experimental asymmetries $(f_np)^+$ and $(f_np)^-$ in equations

$$\sigma^{\pm}_{pf_n}=\sigma_p[1+(f_np)^{\pm}], \qquad (3)$$

were fitted separately for the + and − helicity TOF spectra. Here $\sigma^{\pm}_{pf_n}$ is the experimental neutron cross section for the + and − neutron helicity states, and f_n is the absolute value of the neutron beam polarization. The value of f_n was determined in a separate study of the well-known longitudinal asymmetry of the 0.75-eV resonance in lanthanum [31]. Although the quantities $(f_np)^+$ and $(f_np)^-$ should differ only by a sign, statistical or systematic uncertainties may introduce an additional difference. The asymmetry p defined by Eq. (1) was calculated as

$$p=\frac{[(f_np)^+-(f_np)^-]}{f_n[2+(f_np)^++(f_np)^-]}. \qquad (4)$$

The PNC amplification parameters $A_{pJ}=\sqrt{\Sigma_s 4(g\Gamma^s_{nJ}/g\Gamma^p_{nJ})/(E_{sJ}-E_{pJ})^2}$ (see Sec. IV) are listed for those p-wave resonances for which the longitudinal asymmetry was measured. The amplification factors depend on the spin J because the weak interaction mixes only those p- and s-wave resonances with the same spin J. For ^{105}Pd there are two entries for A_J for all resonances for which the longitudinal asymmetry was measured, corresponding to the two possible spins for which the ''weak mixing'' is possible. (The spins of the p-wave resonances are unknown.) For the spin-zero isotopes, the amplification factors are listed only for the spin-1/2 p-wave resonances, since in this case weak mixing is possible only for spin-1/2 resonances. The analysis to determine the PNC asymmetries in palladium was performed on the summed data. The values of the longitudinal asymmetries p are listed for four palladium isotopes in Tables I–IV.

IV. ANALYSIS

A detailed description of the analysis of the PNC cross section asymmetries is given by Bowman *et al.* [32]. An example of the application of this analysis method for $I=0$ targets is given in our study of uranium [9] and an example of the method for $I\neq0$ targets in our study of silver [12]. A key point is that the observed PNC effect in the p-wave

TABLE II. Resonance parameters and PNC asymmetries p for ^{105}Pd. The parameters A_J have dimensions eV^{-1}.

E (eV)	l	J^a	$g\Gamma_n$ (meV)	A_2	A_3	p (%)	$\lvert p\rvert/\Delta p$
-6.07[a]	0	3	$0.95\sqrt{E}$				
3.91[b]	1		0.00046 ± 0.00003				
11.78[a]	0	3	0.105 ± 0.001				
13.22	0	2	1.33 ± 0.05				
24.49[b]	0		0.080 ± 0.05				
25.10	0	3	1.79 ± 0.05				
27.59[b]	1		0.0032 ± 0.0003				
30.05[a]	0	2	0.180 ± 0.002				
38.43	0	3	0.189 ± 0.009				
41.19[b]	1		0.0053 ± 0.0002	2.9	7.5	-0.06 ± 0.24	0.3
42.56	0		0.033 ± 0.001				
44.39[b]	1		0.0079 ± 0.0003	2.4	5.5	0.25 ± 0.16	1.6
49.93[b]	1		0.0021 ± 0.0001				
55.23	0	3	3.9 ± 0.1				
68.3	0	3	0.92 ± 0.03				
72.5[b]	1		0.0139 ± 0.0006	9.1	5.8	0.59 ± 0.066	9.8
77.7	0	2	7.8 ± 0.2				
79.5[b]	1		0.0139 ± 0.0007	27.2	7.7	-0.072 ± 0.043	1.7
80.5[b]	1		0.033 ± 0.001	11.1	5.8	-0.02 ± 0.078	0.3
82.9[b]	1		0.032 ± 0.001	6.2	9.4	0.21 ± 0.05	4.2
83.3[b]	1		0.039 ± 0.002	5.1	9.4	0.18 ± 0.047	4.5
86.7	0	3	10.2 ± 0.3				
94.3[b]	1		0.008 ± 0.001				
101.2	1		0.028 ± 0.001	2.2	4.7	-0.154 ± 0.093	1.7
104.0	0	3	0.72 ± 0.03				
113.5[b]	1		0.007 ± 0.001				
116.9	1		0.036 ± 0.002	2.3	2.2	-0.14 ± 0.11	1.3
126.2	0	3	1.88 ± 0.06				
130.5	1		0.044 ± 0.002	3.6	3.3	0.21 ± 0.12	1.8
132.5[b]	1		0.025 ± 0.001	5.4	3.2	0.27 ± 0.31	0.9
134.1	1		0.122 ± 0.005	2.8	1.2	-0.07 ± 0.70	0.1
136.5	1		0.026 ± 0.001	8.2	2.3	0.40 ± 0.30	1.3
141.1[a]	0	2	5.75 ± 0.5				
144.4[b]	1		0.019 ± 0.001	18.1	2.7	0.17 ± 0.50	0.3
147.8[b]	1		0.158 ± 0.007	13.2	1.2	0.30 ± 0.25	1.2
150.0	0	2	32.6 ± 1.0				
154.6	0	3	2.07 ± 0.08				
158.70	0	2	3.5 ± 0.1				
161.0[b]	1		0.026 ± 0.001	12.3	3.4	0.061 ± 0.60	1.6
165.9[b]	1		0.040 ± 0.002	4.9	4.3	-0.11 ± 0.35	0.3
168.2	0	3	0.87 ± 0.04				
170.7	1		0.082 ± 0.004	2.8	2.7	0.08 ± 0.20	0.4
183.9	0	2	7.7 ± 0.4				
202.5	0	2	5.6 ± 0.2				
208.3	1		0.057 ± 0.002	3.8	1.3	-0.24 ± 0.27	0.9
215.4	1		0.103 ± 0.004	1.6	1.4	-0.20 ± 0.21	1.0
222.6[b]	1		0.049 ± 0.002	2.0	4.5	0.90 ± 0.52	1.7
226.8	0	3	4.0 ± 0.1				
230.4[b]	1		0.050 ± 0.002	2.0	5.3	0.06 ± 0.50	0.1
251.4	0	2	3.0 ± 0.1				
252.4[a]	0	3	19.8 ± 0.25				
260.0	0	2	22.4 ± 0.7				
268.3[b]	1		0.116 ± 0.005	3.4	1.8	-0.30 ± 0.29	1.0
286.8[a]	0	3	3.15 ± 0.10				
305.1	0	2	53.3 ± 1.7				
311.0[b]	1		0.057 ± 0.003				
313.3	0	2	2.05 ± 0.09				
322.1[a]	1		0.072 ± 0.003				

[a]Values from Ref. [29].

[b]New resonances that are not listed in the latest compilation [30].

TABLE III. Resonance parameters and PNC asymmetries p for ^{106}Pd. The parameter A_J has dimensions eV^{-1}.

E (eV)	l	J	$g\Gamma_n$ (meV)	A_J	p (%)	$\lvert p\rvert/\Delta p$
63.47[a]	1		0.013±0.001	1.6	0.07±0.07	1.0
146.4[a]	1		0.60±0.03	0.4	0.02±0.08	0.3
156.9[a]	1		0.27±0.01	0.7	−0.16±0.046	3.5
281.5	0	0.5	515±14			
299.8[a]	1		0.24±0.01	5.8	0.09±0.15	0.6
406.4[a]	1		0.83±0.03	0.5	−0.07±0.12	0.6
461.9[a]	1		1.16±0.04	0.3	−0.04±0.12	0.3
521.9[a]	1		6.0±0.3	0.1	−0.06±0.06	1.0
562.5[a]	1		5.5±0.2	0.1	−0.04±0.07	0.6
593.4[a,b]	(1)		12.5±0.6	0.1	−0.17±0.04	4.2
644.9[a]	1		0.52±0.05	0.5	0.60±0.38	1.6
870.6[a]	0	0.5	877±30			
922.0[a]	0	0.5	705±26			
967.5	1		16±1	0.4	0.12±0.07	1.7
1005[a]	0	0.5	58±4			
1148[a]	1		4.0±0.4	0.2	0.58±0.24	2.4
1206[a]	1		10.0±0.7	0.1	−0.11±0.15	0.7
1306[a]	1		3.4±0.3	0.2	0.36±0.40	0.9
1323[a]	1		7.8±0.8	0.2	−0.17±0.21	0.8
1377[a]	1		2.2±0.2	1.0	−0.53±0.66	0.8
1398[a]	0	0.5	231±17			
1511[a]	1		28±2	0.1	0.09±0.12	0.8
1557[a]	1		1.7±0.2	0.7	−1.2±1.2	1.0
1585[a]	0	0.5	158±16			
1597[a]	1		12±1	0.6	−0.17±0.22	0.8
1624[a]	1		10±1	0.2	−0.12±0.28	0.4
1764[a]	1		18±2	0.2	−0.15±0.21	0.7
1839[a]	0	0.5	914±67			

[a]New resonances.
[b]Possible doublet.

resonance in question is due to contributions from a number of neighboring s-wave resonances. Since there are several mixing matrix elements but only one measured asymmetry, one cannot obtain the individual matrix elements. However, if the weak matrix elements connecting the opposite parity states are random variables, then the longitudinal asymmetry is also a random variable. The variance M^2 of the weak matrix elements—the mean square matrix element of the PNC interaction—can be determined from the distribution of the asymmetries. The analysis depends on the spectroscopic parameters. Our approach to the likelihood analysis is to include all available spectroscopic information and then to average over any remaining unknowns. Additional spectroscopic information reduces the uncertainty in the rms value of the weak matrix element. However, in practice the major contribution to the uncertainty in the rms weak matrix element arises from statistical limitations—the small sample size. Since we usually observe only a very few PNC effects per nuclide, the resulting likelihood distribution is broad.

The observed asymmetry for a given p-wave level μ has contributions from a number of s-wave levels ν, and the PNC asymmetry is

$$p_\mu = 2\sum_\nu \frac{V_{\nu\mu}}{E_\nu - E_\mu}\frac{g_\nu g_{\mu_{1/2}}}{\Gamma_{\mu_n}}, \tag{5}$$

where $g_{\mu_{1/2}}$ and g_ν are the neutron decay amplitudes of levels μ and ν ($g_\mu^2 = g_{\mu_{1/2}}^2 + g_{\mu_{3/2}}^2 \equiv \Gamma_{\mu_n}$ and $g_\nu^2 \equiv \Gamma_{\nu_n}$), E_μ and E_ν are the corresponding resonance energies, and $V_{\nu\mu}$ is the matrix element of the PNC interaction between levels μ and ν. In the following we assume that the total neutron widths and the resonance energies are known.

For targets with $I^\pi = 0^+$, the s-wave resonances have $1/2^+$ and the p-wave resonances $1/2^-$ or $3/2^-$. Only the 1/2 resonances can mix and show parity violation. First consider the likelihood function when $I=0$ and the spins of the p-wave resonances are known. Therefore one analyzes only the data for spin $J=1/2$ resonances. The values of the asymmetries measured for different p-wave resonances are assumed to have mean zero and to be statistically independent. The likelihood function for several resonances is therefore the product of their likelihood functions.

The mean square matrix element M_J^2 is the variance of the

TABLE IV. Resonance parameters and PNC asymmetries p for ^{108}Pd. The parameter A_J has dimensions eV^{-1}.

E (eV)	l	J	$g\Gamma_n$ (meV)	A_J	p (%)	$\lvert p\rvert/\Delta p$
2.96[a]	1	1.5	0.00504±0.00005			
32.98	0	0.5	123±4			
90.98	0	0.5	214±6			
112.7	1		1.03±0.05	1.4	0.04±0.04	1.0
149.8	1		0.060±0.006	2.6	0.06±0.30	0.2
302.7	1		3.70±0.15	0.22	0.03±0.06	0.5
410.6	1		0.69±0.02	2.9	−0.22±0.25	0.9
426.6	0	0.5	371±11			
480.3	1		0.62±0.02	1.0	0.03±0.30	0.1
544.4	1		5.6±0.3	0.25	−0.04±0.09	0.4
635	0	0.5	396±12			
642	1		1.3±0.1	5.1	0.37±0.34	1.1
797	1		6.3±0.4	0.21	0.12±0.14	0.8
843	1		1.3±0.1	0.69	−0.45±0.65	0.7
905	0	0.5	585±29			
955	0	0.5	877±37			
962[a]	0	0.5	47.1±0.4			
1082	1		17±1	0.15	0.09±0.12	0.7
1121[b]	1		0.51±0.05	0.86	0.7±2.3	0.3
1140[b]	1		0.08±0.02	2.4	−5.0±5.7	0.9
1215	0	0.5	418±42			
1359	1		28±2	0.10	0.03±0.14	0.2
1433	0	0.5	148±15			
1456	1		4.5±0.5	0.54	0.45±0.54	0.8
1505[b]	1		0.33±0.05	1.1	−1.2±5.2	0.2
1523	1		2.8±0.3	0.39	−0.11±0.93	0.1
1652	0	0.5	1269±127			
1710	0	0.5	77±8			
1743[b]	1		0.47±0.07	1.5	−8.7±4.9	1.8
1815[b]	1		2.4±0.2	0.37	1.2±1.8	0.7
2010	0	0.5	696±70			
2118	1		7.5±0.8	0.19	0.23±0.81	0.3
2165[b]	1		2.6±0.3	0.24	0.4±2.5	0.2
2287	1		37±4	0.04	−0.31±0.29	1.1

[a]Resonance parameters from [29].
[b]New resonances.

distribution of the individual PNC matrix elements $V_{\nu\mu}$. The quantity p_μ in Eq. (5) is a sum of Gaussian random variables $V_{\nu\mu}$ each multiplied by fixed coefficients, and is itself a Gaussian random variable [33]. The variance of p_μ is $(A_\mu M_J)^2$, where

$$A_\mu = \sqrt{\sum_\nu A_{\nu\mu}^2}, \quad A_{\nu\mu}^2 = \left(\frac{2}{E_\nu - E_\mu}\right)^2 \frac{\Gamma_\nu}{\Gamma_\mu}. \tag{6}$$

The probability density function of the longitudinal asymmetry p is

$$P(p|M_J A) = \frac{1}{\sqrt{2\pi} M_J A} \exp\left(-\frac{p^2}{2M_J^2 A^2}\right) \equiv G(p,(M_J A)^2), \tag{7}$$

where G represents a Gaussian function.

If the experimental asymmetry is p_μ and the *a priori* distribution of the rms matrix element is $P^0(1/2)$, then

$$L(M_{1/2}) = P^0(1/2) \prod_{\mu=1}^{N} P(p_\mu | M_{1/2} A_\mu, \sigma_\mu), \tag{8}$$

and one obtains the final expression

$$L(M_{1/2}) = P^0(1/2) \prod_{\mu=1}^{N} G(p_\mu, (M_{1/2} A_\mu)^2 + (\sigma_\mu)^2). \tag{9}$$

If the p-wave resonance spins are unknown, then there is one term for the spin-1/2 resonances that *can* show parity violation and one term for the spin-3/2 resonances that *can-*

not show parity violation. One weights the two terms according to the level density. The likelihood function is the sum of the two terms:

$$L(M_{1/2}) = P^0(1/2) \prod_{\mu=1}^{N} [p(1/2) G(p_\mu, (M_{J=1/2} A_\mu)^2 + \sigma_\mu^2) + p(3/2) G(p_\mu, \sigma_\mu^2)], \quad (10)$$

where $p(1/2)$ and $p(3/2)$ are the probabilities that $J=1/2$ and $J=3/2$, respectively. The relative probabilities $p(J)$ are estimated using the standard statistical model prescription for the J dependence; see, for example, the discussion by Bowman *et al.* [32]. Of course when J is known then the probability vanishes except for the one known J value.

The likelihood function in Eq. (10) is not normalizable unless $P_{M_J}(M_J)$ goes to zero for large $M_{1/2}$. This difference is due to the $J=3/2$ terms, which are independent of $M_{1/2}$ and lead to a divergent normalization integral. In practice we assume that the prior $P^0(\Gamma_w)$ is a constant up to some value and zero above this value. Since we have measured weak spreading widths in a number of nuclei, we know that the weak spreading width is unlikely to be more than about 5×10^{-7} eV. For the present calculations we used a constant prior below 10×10^{-7} eV and zero above this value. In this method one directly determines the rms matrix element.

The uncertainties on Γ_w were obtained by the method of Eadie *et al.* [33] of evaluating the confidence interval by solving the equation

$$\ln\left[\frac{L(\Gamma_w^{\pm})}{L(\Gamma_w^*)}\right] = -\frac{1}{2}, \quad (11)$$

where Γ_w^* is the most likely value and $\Gamma_w^{\pm}$ gives the confidence range.

The problem for $I \neq 0$ targets is much more complicated. For ^{105}Pd with $I=5/2$, s-wave resonances can be formed with spin 2 or 3, while the p-wave states can have spins 1, 2, 3, or 4. Only the spin 2 and 3 states can show parity violation. Since the rms PNC matrix element M may depend on J, we label the matrix element as M_J. In the absence of spin information we assume that the spreading width is independent of J and fit directly to the spreading width.

If the spins of all s-wave resonances are known, but not the spins of the p-wave levels, then the factor A_μ can be evaluated if the p-wave spin is assumed. $A_\mu = A_\mu(J)$ depends on the spin sequence assumed because only those s-wave levels with the same spin as the p-wave level mix to produce parity violation. The likelihood function is obtained by summing over p-wave level spins, which parallels the procedure for $I=0$.

The entrance channel neutron $j=3/2$ and $j=1/2$ amplitudes are essentially always unknown. This uncertainty is accounted for statistically by using the average value of the ratio of $S^1_{3/2}$ and $S^1_{1/2}$ strength functions, which is described by the parameter a ($a=1.00$ for palladium [34]).

Due to the different level densities D_J, the rms PNC matrix element may be different for $J = I \pm 1/2$ states. We assume that Γ_w is independent of J. The likelihood function can be expressed as a function of the weak spreading width,

$$L(\Gamma_w) = P^0(\Gamma_w) \prod_{\mu=1}^{N} \left[\sum_{J=I\pm 1/2} p(J) P_p^I(p_\mu | M_J A_\mu(J), a, \sigma_\mu) + \sum_{J=I\pm 3/2} p(J) G(p_\mu, \sigma_\mu^2) \right], \quad (12)$$

where M_J should be written as a function of the weak spreading width

$$\Gamma_w = 2\pi (M_J)^2 / D_J. \quad (13)$$

Once Γ_w is determined, the weak matrix element M is obtained directly from this equation. Since the level densities for $J=2$ and $J=3$ are not very different and have appreciable uncertainties, we use the average level density and quote only one value of M.

In order to be consistent, one should use the weak spreading width as the variable throughout, and transform the *prior* according to $P^0(\Gamma_w) = P^0(M_J(\Gamma_w)) dM_J(\Gamma_w)/d(\Gamma_w)$. The change of the argument and the *prior* does not change the final (most likely) value of the matrix element, but does change the corresponding errors because of the nonlinear relationship of the variables M_J and Γ_w. Thus for $I \neq 0$, usually one *must* formulate the problem in terms of the spreading width, and then determine the weak matrix element from the spreading width. (The only exception is when there is complete spin information.) This contrasts with the approach for $I=0$, where one determines directly the most likely value of the rms matrix element, and then calculates Γ_w from the known matrix element and the level density.

V. RESULTS

Parity violating asymmetries were observed in ^{104,105,106}Pd. For the even-even palladium isotopes, the level spacings are about 200 eV, or about 10 times larger than the spacings for the heavy even-even nuclides ^{232}Th and ^{238}U that we studied earlier [8,9]. Therefore one expects the size of the PNC effects to be correspondingly smaller. ^{104}Pd showed one statistically significant PNC asymmetry, ^{106}Pd two asymmetries, and ^{108}Pd no asymmetries.

The results for ^{106}Pd require special consideration. There is a 3.5σ asymmetry in a weak p-wave resonance at 156.9 eV and a 4σ asymmetry in a strong resonance at 593.4 eV. The orbital angular momentum of the latter resonance is uncertain, since it has nearly equal probability to occur in Porter-Thomas distributions of neutron widths for s- and p-wave resonances. The PNC asymmetry (assuming the p-wave assignment) for this resonance alone yields a weak matrix element of 10.9 meV [35] and a weak spreading width nearly an order of magnitude larger than any observed in 15 other nuclei. The experimental results for M and Γ_w are listed in Table V for the nuclei studied by the TRIPLE Collaboration. The PNC asymmetry in the 156.9-eV resonance alone gives a smaller and more reasonable value of M_J. The simplest explanation is the existence of a doublet of p- and

TABLE V. TRIPLE results on level spacings, weak matrix elements and spreading widths.

A	D_J (eV)	M_J (meV)	Γ_w (10^{-7}eV)	Reference
^{93}Nb	190±16	⩽0.6	⩽0.1	[10]
^{103}Rh	60±5	$1.2^{+0.5}_{-0.4}$	$1.4^{+1.2}_{-0.6}$	[11]
^{104}Pd	220±65	$2.3^{+3.3}_{-1.1}$	$1.5^{+6.8}_{-1.1}$	a
^{105}Pd	24±2	$0.6^{+0.3}_{-0.2}$	$0.8^{+1.3}_{-0.5}$	a
^{106}Pd	217±61	$1.9^{+1.8}_{-0.9}$	$1.0^{+2.8}_{-0.7}$	a
^{107}Ag	33±4	$1.2^{+0.5}_{-0.3}$	$2.7^{+2.6}_{-1.2}$	[12]
^{109}Ag	28±3	$0.8^{+0.5}_{-0.3}$	$1.3^{+2.5}_{-0.7}$	[12]
^{113}Cd	33±4	$1.3^{+0.6}_{-0.4}$	$3.2^{+3.4}_{-1.6}$	[13]
^{115}In	22±1	$0.7^{+0.2}_{-0.1}$	$3.2^{+3.4}_{-1.6}$	[14]
^{117}Sn	79±6	$0.6^{+0.4}_{-0.2}$	$0.3^{+0.6}_{-0.2}$	[15]
^{121}Sb	25±3	$1.4^{+0.9}_{-0.5}$	$4.8^{+8.6}_{-2.9}$	[16]
^{123}Sb	60±7	$1.3^{+2.7}_{-0.7}$	$1.9^{+15}_{-1.4}$	[16]
^{127}I	23±3	$0.5^{+0.3}_{-0.2}$	$0.6^{+0.9}_{-0.4}$	[16]
^{133}Cs	41±4	$0.06^{+0.25}_{-0.02}$	$0.006^{+0.018}_{-0.004}$	[17]
^{232}Th	17±2	$1.1^{+0.3}_{-0.2}$	$4.7^{+2.7}_{-1.8}$	[8]
^{238}U	21±3	$0.7^{+0.3}_{-0.2}$	$1.3^{+1.0}_{-0.6}$	[9]

[a]Present work.

s-wave resonances at 593 eV. Since there is no information concerning the energy separation and the strengths of the doublet components, the PNC information obtained from the 593-eV resonance was omitted from the subsequent analysis.

For the even-even palladium isotopes the analysis is straightforward and one can determine the weak matrix element directly. However, since there are only a few statistically significant effects, the uncertainties are large. The weak matrix elements are $(2.3^{+3.1}_{-1.1})$ meV for ^{104}Pd and $(1.9^{+1.8}_{-0.9})$ meV for ^{106}Pd. The corresponding spreading widths are $\Gamma_w=(1.5^{+6.8}_{-1.1})\times10^{-7}$ eV for ^{104}Pd and $\Gamma_w=(1.0^{+2.8}_{-0.7})\times10^{-7}$ eV for ^{106}Pd.

For ^{105}Pd the longitudinal asymmetries were measured for 23 *p*-wave resonances. There are three statistically significant PNC asymmetries. The 9σ effect at 72.5 eV is straightforward. However, near 83.1 eV there are two *p*-wave resonances, as is clear in Fig. 2. The width of the transmission dip near 83.1 eV is wider than the width of the resonance at 72.5 eV. The results listed in Table II are obtained assuming resonances at 82.9 and 83.3 eV. The spins of the *s*-wave resonances are known, but the spins of the *p*-wave resonances are not. Since there was no information about the *p*-wave spins, the likelihood analysis was performed using Eq. (12). The likelihood function for ^{105}Pd is shown in Fig. 3. The value for the weak spreading width is $\Gamma_w=(0.8^{+1.3}_{-0.5})\times10^{-7}$ eV, which corresponds to a weak matrix element $M_J=(0.6^{+0.3}_{-0.2})$ meV.

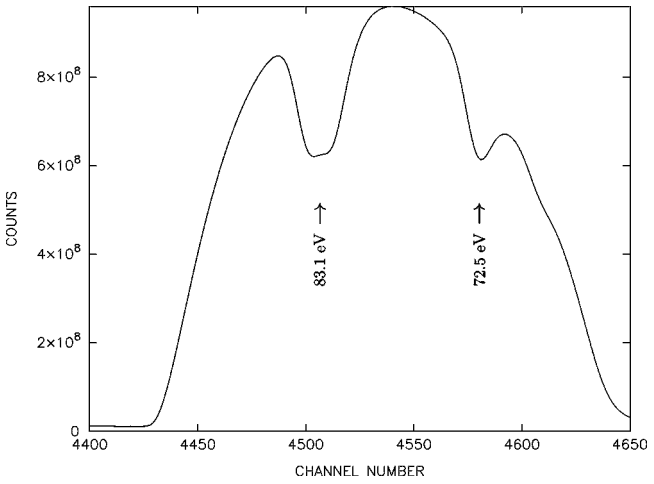

FIG. 2. Neutron resonances in ^{105}Pd. There is a *p*-wave doublet near 83.1 eV and a single *p*-wave resonance at 72.5 eV. All three of these *p*-wave resonances show parity violation.

VI. SUMMARY AND CONCLUSION

PNC asymmetries were measured via the transmission method on a natural palladium target. Many new resonances were observed in the transmission spectrum, primarily *p*-wave resonances. Many of the new resonances are in the odd mass isotope ^{105}Pd, due to its higher level density. However, since there are four primary even-even isotopes (^{104,106,108,110}Pd) the assignment of these new resonances required studies of isotopically enriched targets. Measurements on these targets were performed with a γ-ray detector array, and the resulting spectroscopy of the palladium isotopes was discussed by Smith *et al.* [15].

For the even isotopes that showed PNC effects (^{104}Pd and ^{106}Pd), the data were analyzed directly in terms of the rms weak matrix element and the weak spreading width determined from Eq. (13). For the odd mass nuclide ^{105}Pd the asymmetries were fitted with the weak spreading width as the free parameter using Eq. (12). The rms weak matrix element was then determined from the spreading width. For ^{104}Pd, ^{105}Pd, and ^{106}Pd the matrix elements are of order ~1 meV and the weak spreading widths are of order $\sim1\times10^{-7}$ eV. As shown in Table V, the values for the

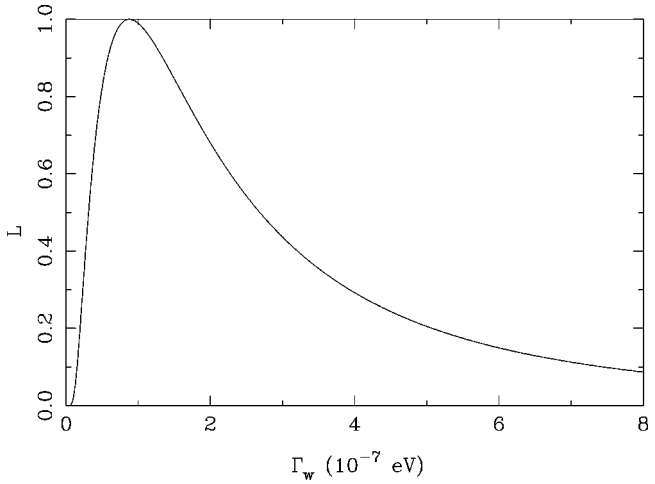

FIG. 3. Plot of the likelihood function for ^{105}Pd. A total of 23 *p*-wave resonances were analyzed and three statistically significant PNC effects were observed. A value of $\Gamma_w=(0.8^{+1.3}_{-0.5})\times10^{-7}$ eV was obtained.

palladium isotopes are typical for this mass region. Except for one anomalously small value (for ^{133}Cs) the set of measured weak spreading widths are consistent with a constant value. A least squares fit yields a best value of $\sim 1.8 \times 10^{-7}$ eV. Therefore the PNC results for the palladium isotopes agree with the larger body of parity violation measurements.

ACKNOWLEDGMENTS

This work was supported in part by the U.S. Department of Energy, Office of High Energy and Nuclear Physics, under Grants No. DE-FG02-97-ER41042 and DE-FG02-97-ER41033, and by the U.S. Department of Energy, Office of Energy Research, under Contract No. W-7405-ENG-36.

[1] E.G. Adelberger and W.C. Haxton, Annu. Rev. Nucl. Part. Sci. **35**, 501 (1985).
[2] V.P. Alfimenkov, S.B. Borzakov, Vo Van Thuan, Yu.D. Mareev, L.B. Pikelner, A.S. Khrykin, and E.I. Sharapov, Nucl. Phys. **A398**, 93 (1983).
[3] J.D. Bowman, G.T. Garvey, Mikkel B. Johnson, and G.E. Mitchell, Annu. Rev. Nucl. Part. Sci. **43**, 829 (1993).
[4] C.M. Frankle, S.J. Seestrom, N.R. Roberson, Yu.P. Popov, and E.I. Sharapov, Phys. Part. Nucl. **24**, 401 (1993).
[5] V.V. Flambaum and G.F. Gribakin, Prog. Part. Nucl. Phys. **35**, 423 (1995).
[6] G.E. Mitchell, J.D. Bowman, and H.A. Weidenmüller, Rev. Mod. Phys. **71**, 445 (1999).
[7] G.E. Mitchell, J.D. Bowman, S.I. Penttilä, and E.I. Sharapov, Phys. Rep. **354**, 157 (2001).
[8] S.L. Stephenson *et al.*, Phys. Rev. C **58**, 1236 (1998).
[9] B.E. Crawford *et al.*, Phys. Rev. C **58**, 1225 (1998).
[10] E.I. Sharapov *et al.*, Phys. Rev. C **59**, 1131 (1999).
[11] D.A. Smith *et al.*, Phys. Rev. C **60**, 045502 (1999).
[12] L.Y. Lowie *et al.*, Phys. Rev. C **59**, 1119 (1999).
[13] S.J. Seestrom *et al.*, Phys. Rev. C **58**, 2977 (1998).
[14] S.L. Stephenson *et al.*, Phys. Rev. C **61**, 045501 (2000).
[15] D.A. Smith *et al.*, Phys. Rev. C **64**, 015502 (2001).
[16] Y. Matsuda *et al.*, Phys. Rev. C **64**, 015501 (2001).
[17] E.I. Sharapov *et al.*, Phys. Rev. C **59**, 1772 (1999).
[18] S.J. Seestrom *et al.*, Nucl. Instrum. Methods Phys. Res. A **433**, 603 (1999).
[19] D.A. Smith *et al.*, Phys. Rev. C **65**, 024607 (2002).
[20] B.E. Crawford *et al.*, Phys. Rev. C **58**, 729 (1998).
[21] P.W. Lisowski, C.D. Bowman, G.J. Russell, and S.A. Wender, Nucl. Sci. Eng. **106**, 208 (1990).
[22] N.R. Roberson *et al.*, Nucl. Instrum. Methods Phys. Res. A **326**, 549 (1993).
[23] J.J. Szymanski *et al.*, Nucl. Instrum. Methods Phys. Res. A **340**, 564 (1994).
[24] S.I. Penttilä, J.D. Bowman, P.P.J. Delheij, C.M. Frankle, D.G. Haase, H. Postma, S.J. Seestrom, and Yi-Fen Yen, in *High Energy Spin Physics*, edited by K.J. Heller and S.L. Smith, AIP Conf. Proc. No. 342 (AIP, New York, 1995), p. 532.
[25] J.D. Bowman, S.I. Penttilä, and W.B. Tippens, Nucl. Instrum. Methods Phys. Res. A **369**, 195 (1996).
[26] Yi-Fen Yen *et al.*, Nucl. Instrum. Methods Phys. Res. A **447**, 476 (2000).
[27] J.D. Bowman, Y. Matsuda, Y.-F. Yen, and B.E. Crawford (unpublished).
[28] C.W. Reich and M.S. Moore, Phys. Rev. **111**, 929 (1958).
[29] S.F. Mughabghab, M. Divadeenam, and N.E. Holden, *Neutron Cross Sections* (Academic Press, New York, 1981), Vol. 1, Part A.
[30] S.I. Sukhoruchkin, Z.N. Soroko, and V.V. Deriglazov, in *Numerical Data and Functional Relationships in Science and Technology*, edited by H. Schopper, Landolt-Börnstein, New Series, Group 1, Vol. 16, Pt. b, (Springer, New York, 1998).
[31] V.W. Yuan *et al.*, Phys. Rev. C **44**, 2187 (1991).
[32] J.D. Bowman, L.Y. Lowie, G.E. Mitchell, E.I. Sharapov, and Yi-Fen Yen, Phys. Rev. C **53**, 285 (1996).
[33] W.T. Eadie, P. Drijard, F.E. James, M. Roos, and B. Sadoulet, *Statistical Methods in Experimental Physics* (North-Holland, Amsterdam, 1971), p. 204.
[34] L.V. Mitsyna, A.B. Popov, and G.S. Samosvat, in *Nuclear Data for Science and Technology*, edited by S. Igarasi (Saikon, Tokyo, 1988), p. 111.
[35] B.E. Crawford *et al.*, Phys. Rev. C **60**, 055503 (1999).